

# Highly efficient siRNA delivery system into human and murine cells using single-wall carbon nanotubes

To cite this article: M S Ladeira *et al* 2010 *Nanotechnology* **21** 385101

View the [article online](#) for updates and enhancements.

## Related content

- [Design of double-walled carbon nanotubes for biomedical applications](#)  
V Neves, E Heister, S Costa *et al*.
- [Hyaluronic acid-fabricated nanogold delivery of the inhibitor of apoptosis protein-2 siRNAs inhibits benzo\[a\]pyrene-induced oncogenic properties of lung cancer A549 cells](#)  
Chung-Ming Lin, Wei-Chien Kao, Chun-An Yeh *et al*.
- [Synthesis and characterization of polyamidoamine dendrimer-coated multi-walled carbonnanotubes and their application in gene delivery systems](#)  
Bifeng Pan, Daxiang Cui, Ping Xu *et al*.

## Recent citations

- [A Review of Theranostics Applications and Toxicities of Carbon Nanomaterials](#)  
Nitin Gupta *et al*
- [Petros Kechagioglou \*et al\*](#)
- [Overview of Carbon Nanotubes for Biomedical Applications](#)  
Juliette Simon *et al*



**IOP | ebooks™**

Bringing you innovative digital publishing with leading voices to create your essential collection of books in STEM research.

Start exploring the collection - download the first chapter of every title for free.

# Highly efficient siRNA delivery system into human and murine cells using single-wall carbon nanotubes

M S Ladeira<sup>1</sup>, V A Andrade<sup>1</sup>, E R M Gomes<sup>1</sup>, C J Aguiar<sup>1</sup>,  
E R Moraes<sup>1</sup>, J S Soares<sup>2</sup>, E E Silva<sup>2</sup>, R G Lacerda<sup>2</sup>, L O Ladeira<sup>2</sup>,  
A Jorio<sup>2</sup>, P Lima<sup>3</sup>, M Fatima Leite<sup>1,4</sup>, R R Resende<sup>2,5</sup> and  
S Guatimosim<sup>1</sup>

<sup>1</sup> Department of Physiology and Biophysics, Federal University of Minas Gerais, Belo Horizonte, MG, 31270-901, Brazil

<sup>2</sup> Department of Physics, Federal University of Minas Gerais, Belo Horizonte, MG, 31270-901, Brazil

<sup>3</sup> Department of Biosystems Engineering, Federal University of São João Del Rei, São João Del Rei, MG, 36307-352, Brazil

<sup>4</sup> Howard Hughes Medical Institute, 4000 Jones Bridge Road, Chevy Chase, 20815-6789 MD, USA

<sup>5</sup> Department of Biochemistry, Federal University of São João Del Rei, Advanced Center of Health, Divinópolis, MG, 35501-296, Brazil

E-mail: [rresende@hotmail.com](mailto:rresende@hotmail.com) and [guatimosim@icb.ufmg.br](mailto:guatimosim@icb.ufmg.br)

Received 29 June 2010

Published 27 August 2010

Online at [stacks.iop.org/Nano/21/385101](http://stacks.iop.org/Nano/21/385101)

## Abstract

Development of RNA interference (RNAi) technology utilizing short interfering RNA sequences (siRNA) has focused on creating methods for delivering siRNAs to cells and for enhancing siRNA stability *in vitro* and *in vivo*. Here, we describe a novel approach for siRNA cellular delivery using siRNA coiling into carboxyl-functionalized single-wall carbon nanotubes (SWCNTs). The CNT–siRNA delivery system successfully demonstrates nonspecific toxicity and transfection efficiency greater than 95%. This approach offers the potential for siRNA delivery into different types of cells, including hard-to-transfect cells, such as neuronal cells and cardiomyocytes. We also tested the CNT–siRNA system in a non-metastatic human hepatocellular carcinoma cell line (SKHep1). In all types of cells used in this work the CNT–siRNA delivery system showed high efficiency and apparent no side effects for various *in vitro* applications.

## 1. Introduction

In recent years, carbon-nanotube-based carriers are one of the non-viral vectors that have gained increasing interest as a safer and cost-effective delivery system for gene materials including plasmid DNA (pDNA) and oligonucleotides (ODN) as well as proteins and peptides. Carbon nanotubes (CNTs) have beneficial qualities such as low toxicity, low immunogenicity (Liu *et al* 2008, Cherukuri *et al* 2006) and biocompatibility (Dubin *et al* 2008). Moreover, they offer the possibility of functionalization that can easily form polyelectrolyte complexes with negatively charged nucleotides by electrostatic interaction. Previously, some studies evaluated the ability

of multi-wall carbon nanotubes (MWCNTs) and single-wall carbon nanotubes (SWCNTs) covalently or electrostatically linked to chemical groups as transfection agents to deliver gene materials including pDNA, ODN, proteins and peptides (Kam *et al* 2005, Rege *et al* 2006, Zhang *et al* 2006, Krajcik *et al* 2008). Previous work using an immortalized HeLa cell line (Kam *et al* 2005) reported a covalent conjugation of siRNA to phospholipid-functionalized SWCNTs via cleavable disulfide linkage. By using this approach they have shown highly efficient delivery of siRNA by SWCNTs, and achieved a more potent RNAi functionality than a widely used commercial agent. By using the same functionalization technique of siRNA conjugation through disulfide linkages specific knockdown of

target gene in T-cells transfected with SWCNTs–siRNA was obtained (Liu *et al* 2007). Interestingly, the authors failed to see a knockdown effect when using liposome-based carriers.

Moreover, another study reported that positively charged –CONH–(CH<sub>2</sub>)<sub>6</sub>–NH<sup>3+</sup>Cl-functionalized SWCNTs were able to bind and efficiently carry siRNA into tumor cells. (Zhang *et al* 2006). Recently, another study used a chemical functionalization of SWCNTs with hexamethylenediamine (HMDA) and poly(diallyldimethylammonium) chloride (PDDA) to bind negatively charged siRNA. PDDA–HMDA–SWCNTs were able to carry siRNA into cardiomyocytes and efficiently knock down targeted genes ERK1 and ERK2. Importantly, the complex PDDA–HMDA–SWCNTs showed no cytotoxic effects on cardiomyocytes (Krajcik *et al* 2008).

Here, we report a new strategy for delivering siRNA into hard-to-transfect cells by using carboxylic-functionalized SWCNTs. To compare the delivery efficiency in a stable cell line, we used the SKHep1 cell culture. We further report that carboxylic-SWCNTs represent an efficient non-cytotoxic system for carrying siRNA.

## 2. Experimental details

### 2.1. Materials

If not otherwise indicated, all reagents were purchased from Sigma.

### 2.2. Carbon nanotube synthesis

SWCNTs were prepared by the arc discharge method using a Co/Ni (0.6/0.6 at.%) catalyst with helium at a total pressure 500 Torr, with the arc generated by a current of 200 A/20 V (Trigueiro *et al* 2007, Da Silva *et al* 2009). After the synthesis, an indispensable as-grown SWCNT purification (~95%) process was performed. One gram of SWCNTs was refluxed with 3 M HNO<sub>3</sub> at 120 °C during 32 h, centrifuged at 7000 rpm and washed with distilled water in order to purify the SWCNTs. Nitric acid oxidation on the carbon nanotubes exhibits a dual role: this treatment was performed to decorate the SWCNT surface with –COOH groups and also to afford short SWCNTs (length 50–500 nm). The final solution was dried during 12 h in an oven at 60 °C. At the end, 0.75 g of high purity COOH-SWCNTs was obtained.

### 2.3. RNAi preparation

For siRNA studies, potential target sites within the rat inositol 1,4,5-triphosphate receptor (InsP3R) genes were selected and then searched with NCBI Blast to confirm specificity for each InsP3R isoform. The siRNAs for the type I and II InsP3R were prepared by a transcription-based method using the Silencer kit according to the manufacturer's instructions (Ambion Inc., Austin, TX). The sense and antisense oligonucleotides of siRNAs were, respectively, as follows: type I, 5'-AAAGTTGTAGCTGCTGGTGCCTCCTGTCCTC-3' and 5'-AAAGCACCAGCAGCTACAA CTCCTGTCCTC-3'; type II, 5'-AACAGCCTAATCAAGATCTCCCCTGTCTC-3' and 5'-AAGGAGATCTTGATTAGGCTGCCTGTCTC-3'.

### 2.4. Transfection solutions

A stable aqueous solution of short single-wall CNTs (~length 200 nm) was prepared with high purity short COOH-SWCNTs dissolved in MilliQ water. The solution was sonicated for 3 h followed by centrifugation (15 700g). 50 or 100 nM of siRNA for each InsP3R isoform was added to 50 μl (dose 1) or 100 μl (dose 2) of a CNT aqueous solution, sonicated for 30 min and added to the cell medium. CNT concentration in the cell's medium was respectively 0.0125 and 0.0250 mg ml<sup>-1</sup>. For RNAi preparation the cells were washed and supplied with 1 ml of fresh tissue culture medium. 50 or 100 nM of siRNA for the InsP3R-II isoform was added to 3 μl (concentration 1) or 6 μl (concentration 2) of transfection reagent (RNAifect, QIAGEN) and then the volume was completed to 100 μl with tissue culture medium. The mixture was incubated for 15 min at 37 °C for complex formation, and then 900 μl of tissue culture medium was added to the mixture and this solution was placed dropwise onto the cells. The cells were incubated at 37 °C in an atmosphere of 5% CO<sub>2</sub> for 48 h prior to use, as previously shown (Mendes *et al* 2005).

### 2.5. SKHep1 cell culture

SKHep1 cells (American Type Culture Collection—Manassas, VA) were cultured in Dulbecco's modified Eagle's medium (DMEM) (GIBCO BRL, Frederick, MD) supplemented with 10% fetal bovine serum and antibiotics. Cells were incubated at 37 °C in an atmosphere of 5% CO<sub>2</sub> for 48 h.

### 2.6. Cardiomyocyte cell culture

Neonatal cardiomyocytes were isolated from hearts of three-day-old Wistar rats, as previously described (Guatimosim *et al* 2008). Briefly, cells were resuspended in DMEM supplemented with 10% fetal bovine serum (FBS) (GIBCO BRL, Frederick, MD), 100 units ml<sup>-1</sup> penicillin, 100 μg ml<sup>-1</sup> streptomycin. Cardiomyocytes were plated into fibronectin-coated culture dishes or flasks and incubated at 37 °C in 5% CO<sub>2</sub> incubator. Two days after plating, cells were rinsed with DMEM and fed for another 24 h with regular culture medium, now including 20 μg ml<sup>-1</sup> cytosine β-D-arabinofuranoside (ARAC) to inhibit growth of non-cardiomyocyte cells. The cultured cardiomyocytes were used in experiments on the fourth day of culture.

### 2.7. Rat dorsal root ganglion (DRG) neuron cell culture

Male Wistar rats (220–280 g) were sacrificed by decapitation, and dorsal root ganglia dissected out and maintained in HEPES-buffered saline (HBS) containing (in mM): NaCl 140, KCl 2.5, Hepes 10, Glucose 7.5, pH adjusted to 7.4 with NaOH. Ganglia were cleaned of connective tissue and sectioned prior to 20 min enzymatic treatment with Papain (1 μg ml<sup>-1</sup>), activated by cystein (0.03 μg ml<sup>-1</sup>) in HBS. The ganglia were washed with enzyme-free HBS followed by 20 min treatment with 2.5 μg ml<sup>-1</sup> collagenase (Type 1A) in HBS. During enzymatic treatment, tubes were gently agitated to avoid settling and adherence of the tissue.

Enzymatic treatment was halted by washing the ganglia with DMEM containing 10% FBS. Digested ganglia fragments were triturated through pipettes fire polished to an inner tip diameter of 2 mm until dissociated. The cell suspension obtained was plated onto glass cover slips previously treated with polylysine (MW 70 000–150 000, 20  $\mu\text{g ml}^{-1}$ , 12 h at 4 °C) followed by laminin (20  $\mu\text{g ml}^{-1}$ , 6 h at 4 °C). The cultures were stored at 37 °C in a 5% CO<sub>2</sub> incubator to allow the cells to settle and adhere to the cover slips.

### 2.8. Immunofluorescence

Immunofluorescence to detect the subcellular distribution of InsP3R isoform was performed, as described previously (Mendes *et al* 2005). Briefly, cardiomyocytes, DRG and SKHep1 cells were fixed in 4% paraformaldehyde, followed by cell permeabilization in 0.5% Triton X-100. After a blocking step, cells were incubated with primary antibody against specific InsP3R isoforms and then rinsed with phosphate-buffered saline and 1% bovine serum albumin. The specimens were then incubated with Alexa 488 secondary antibody (Invitrogen) and/or co-labeled with Alexa 633 (Invitrogen). A Zeiss LSM 510 confocal microscope (Thorwood, NY) was used for all imaging studies. Images were obtained by excitation at 488 nm and observation at 505–550 nm to detect Alexa 488. Each InsP3R isoform was labeled using isoform-specific antibodies. Type I InsP3R antibodies were from affinity-purified specific rabbit polyclonal antiserum directed against the 19 C-terminal residues of the mouse type I InsP3R (Hagar *et al* 1998) and were produced by Research Genetics (Huntsville, AL). Type II InsP3R antibodies were from affinity-purified specific rabbit polyclonal antiserum directed against the 18 C-terminal residues of the rat type II InsP3R (Wojcikiewicz 1995) and were kindly provided by Richard Wojcikiewicz (SUNY, Syracuse, NY).

### 2.9. RNA extraction, reverse transcription and real-time PCR

cDNA templates were amplified by real-time PCR on the 7000 Sequence Detection System (ABI Prism, Applied Biosystems, Foster City, CA) using the Syber green method as described (Resende *et al* 2008, Soares *et al* 2007). Sets of primers were chosen for type II InsP3R, forward, 5' AGCACATTACGGCGAATCCT 3' and reverse 5' CCTGACAGAGGTCGGTTCACA 3', and type III InsP3R, forward 5' CGGAGCGCTTCTTCAAGGT 3' and reverse 5' TGACAGCGACCGTGGACTT 3', and type II RyR, forward 5' CCGCATCGACAAGGACAAA 3' and reverse 5' TGAGGGCTTTTCTGAGCAT 3', and for  $\beta$ -actin, forward 5' GACGGCCAGGTCATCACTATTG 3' and reverse 5' AGGAAGGCTGGAAAAGAGCC 3' to give PCR products less than 100 base pairs in length. Primers and probes were custom synthesized by Integrated DNA Technologies (Coralville, IA).

Gene expression profile in SKHep1 cells incubated or not with SWCNTs (0.0250 mg ml<sup>-1</sup>) was performed with primers selected and searched with NCBI Blast to confirm specificity. Genes were selected for: G1/S phase-associated genes (cyclin

D1, cyclin D2, cdk4, cyclin E1, cyclin E2, and cdk2), S phase-associated genes (cyclin A1, and cdk2), G2 phase-associated genes (cyclin A2, and cyclin D3), M phase-associated genes (cyclin B1, and cyclin B2), cell cycle inhibitors such as p16INK4a, p15INK4b and p19INK4d. A panel of apoptotic (p53, Apaf-1, caspase 6 and bax) and anti-apoptotic genes (mdm2, p21CIP/WAF) were also chosen for this study.

Total RNA from SKHep1 cells was isolated using the TRIzol reagent (Invitrogen). Contaminating DNA was removed by DNase I (Ambion Inc., Austin, TX) treatment and integrity of the isolated RNA was analyzed on a 2% SYBR<sup>®</sup> safe DNA-stained agarose gel (Invitrogen, Carlsbad, CA). Three micrograms of total RNA from each sample were used in each case as template for cDNA synthesis in the presence of 50 ng of random primers and 200 units of RevertAid<sup>™</sup> H Minus Moloney murine leukemia virus reverse transcriptase (Fermentas Inc., Hanover, MD) in a total volume of 20  $\mu\text{l}$  for 45 min at 42 °C. Complementary DNA was amplified in a 10  $\mu\text{l}$  volume containing 6  $\mu\text{l}$  of 2x TaqMan Universal PCR Master Mix (Applied Biosystems, Foster City, CA), 100 nM probe (Applied Biosystems, Foster City, CA) and 300 nM of each primer. After a denaturing step at 95 °C for 10 min, 50 cycles were performed at 95 °C for 15 s and then 60 °C for 1 min. Mathematical analysis of the results was performed as recommended by the manufacturer.

### 2.10. Measurement of beating frequency

Cells were loaded with the fluorescent Ca<sup>2+</sup> dye Fluo/4 AM and beating frequency was acquired with a Zeiss LSM 510 confocal microscope (Guatimosim *et al* 2008).

### 2.11. Live/dead cell viability assay

Viability assay was performed in neonatal cardiomyocytes with a live/dead assay kit from Invitrogen (Invitrogen, Carlsbad, CA). Cell medium was removed and cells were washed twice with PBS, and 2 ml of Hepes solution containing 0.5  $\mu\text{l}$  of calcein AM and 1.0  $\mu\text{l}$  of ethidium homodimer was added in each cell well and stored for 30 min at 37 °C in a 5% CO<sub>2</sub> incubator. Live and dead cells were observed with a BioRad MRC-1024 confocal microscope (Hercules, CA). Values were expressed as the number of living cells divided by the total number of cells. All experiments were carried out in triplicate.

### 2.12. Flow cytometry

SKHep1 cells were analyzed by a Becton-Dickinson FAC-Scan instrument after incubation with COOH-SWCNTs (0.0250 mg ml<sup>-1</sup>) for 6, 12, 24 or 48 h. The cells were washed, trypsinized to detach them from the plate surface and washed with PBS, followed by 2 min centrifugation (1000 rpm). Anexin-V-FITC (50  $\mu\text{g ml}^{-1}$ ) and propidium iodide (100  $\mu\text{g ml}^{-1}$ ) were added to the cell in the presence of the binding buffer and allowed to react for 10 min at room temperature. The data presented here represent the mean fluorescence obtained from a population of 50 000 cells.

### 2.13. Raman spectrophotometry

Confocal Raman measurements were performed on an inverted optical microscope with the addition of an  $x, y$  stage for raster-scanning samples. The sample was excited with an He–Ne laser (632.8 nm), focused onto the surface of the sample using an oil objective with 60 $\times$  magnification, NA = 1.4. The Raman scattered light was recorded using: (i) a single-photon counting avalanche photodiode (APD) filtered at the frequency of the CNT G band (1580  $\text{cm}^{-1}$ ) for Raman imaging and (ii) a spectrograph with a charge-coupled device (CCD) for spectral information.

## 3. Results

Here we showed an examination of CNT properties by checking simultaneously its biocompatibility and efficiency as an siRNA delivery method. In this study, we used three distinct cell types (DRG, neonatal cardiomyocytes and SKHep1 cells) in order to evaluate the potential of purified short SWCNTs as siRNA carriers. An effort was made in order to select cell types with distinct characteristics to investigate the physiological potential of CNTs as transfection agents for clinical therapy. In addition, these cells express different isoforms of InsP3R. Moreover, cardiomyocytes and dorsal root ganglion (DRG) neuron cells have in common the feature of being hard to transfect, which has limited their use in siRNA studies. For siRNA experiments the target gene of choice was the InP3R.

### 3.1. Effects of CNTs on cell viability

SKHep1 cells are a liver-derived epithelial cell line, capable of proliferating, that are not polarized. These cells express two different types of InsP3Rs, type II and type III (Leite *et al* 2002), therefore representing a valuable model to investigate the cytotoxicity and specificity of CNT–siRNA complexes.

A critical aspect that plays an important role in determining CNT toxicity is related to its biocompatibility. Therefore, we first evaluated the effect of CNTs on gene expression levels of regulators of cell cycle and apoptosis control factors in SKHep 1 cells. For that, cells were treated with a solution of functionalized CNTs (carboxylic-SWCNTS 0.0250  $\text{mg ml}^{-1}$ ) for 48 h and gene expression levels were evaluated by real-time PCR. Table 1 shows mRNA levels of a panel of 21 genes assessed by real-time PCR. Gene list includes regulators of cell cycle, pro-apoptotic and inhibitor of apoptosis genes. The analyses showed that regulators of cell cycle genes G1/S phase-associated genes (cyclin D1, cyclin D2, cdk4, cyclin E1, cyclin E2, and cdk2), S phase-associated genes (cyclin A1, and cdk2), and G2 phase-associated genes (cyclin A2) were up-regulated, while M phase-associated genes (cyclin B1, and cyclin B2) were down-regulated, suggesting that SKHep1 cells were arrested in the G1 phase in the presence of CNTs. Both apoptosis-related genes such as p53, Apaf-1, caspase 6 and bax, and anti-apoptotic genes (p21CIP/WAF, mdm2, p19ARF) were up-regulated suggesting that SWCNTs do not induce apoptosis in SKHep1 cells.

To investigate the functional consequence of these changes in mRNA levels, we performed FACS in SKHep 1 cells

**Table 1.** Effects of CNTs on mRNA relative expression levels of regulators of cell cycle and apoptosis-related genes.

Genes	Control	CNT
Cyclin A1	1.87	2.61
Cyclin A2	1.70	2.60
Cyclin B1	1.60	0.76
Cyclin B2	1.43	0.74
Cyclin D1	5.34	30.69
Cyclin D2	110.36	250.83
Cyclin D3	1.08	0.99
Cyclin E1	7.90	162.42
Cyclin E2	6.87	122.11
cdk2	2.33	11.91
cdk4	3.90	6.22
p15INK	2.90	1.95
p16INK	1.015	1.47
p19INK	0.95	0.32
p53	1.14	3.07
p21CIP/WAF	0.91	16.41
Apaf-1	0.99	1.48
Caspase6	0.83	1.09
Bax	1.23	1.80
mdm2	0.53	1.36
p19ARF	0.70	0.73

exposed or not to functionalized CNTs (0.0250  $\text{mg ml}^{-1}$ ). As shown in figures 1(A) and (B) no significant difference was observed between untreated control cells and cells incubated with functionalized CNTs at the different exposure times tested (6, 12, 24 and 48 h).

In this study, therefore, we expanded previous findings by showing that CNTs do not affect cellular viability. Although gene expression levels of important cellular pro-apoptotic genes and cell cycle regulators were altered in SKHep 1 cells exposed to CNTs, we also noted a higher expression of survival genes, which may have compensated the increased expression of death genes. This data was confirmed by FACS, which showed no effect of CNTs on SKHep 1 cell viability. These data correlated with findings from a previous study (Shi Kam *et al* 2004) showing that the uptake of SWCNTs did not adversely affect HL60 cells at equivalent CNT concentration used in this work. Taken together, our data show that, although functionalized CNTs alter gene expression, these changes do not lead to reduced cellular viability. Next, we assessed the potential of SWCNTs as siRNA carriers.

### 3.2. SWCNT–siRNA complex efficiently reduces InsP3R expression levels in SKHep1 cells

$\text{Ca}^{2+}$  regulates multiple processes within an individual cell. Among intracellular  $\text{Ca}^{2+}$  channels the InsP3R family is widely expressed in excitable as well as non-excitable cells. In SKHep1 cells, for instance, InsP3Rs are distributed throughout the cytosol and the nucleus (Echevarria *et al* 2003, Mendes *et al* 2005) and  $\text{Ca}^{2+}$  signaling depends entirely on InsP3R-generated  $\text{Ca}^{2+}$  signals. Therefore, we next investigated the efficiency of our CNT–InsP3R–siRNA complex in SKHep1 cells. To achieve maximum effectiveness of exogenously introduced siRNAs, transfection optimization experiments are required, since failure to optimize critical transfection

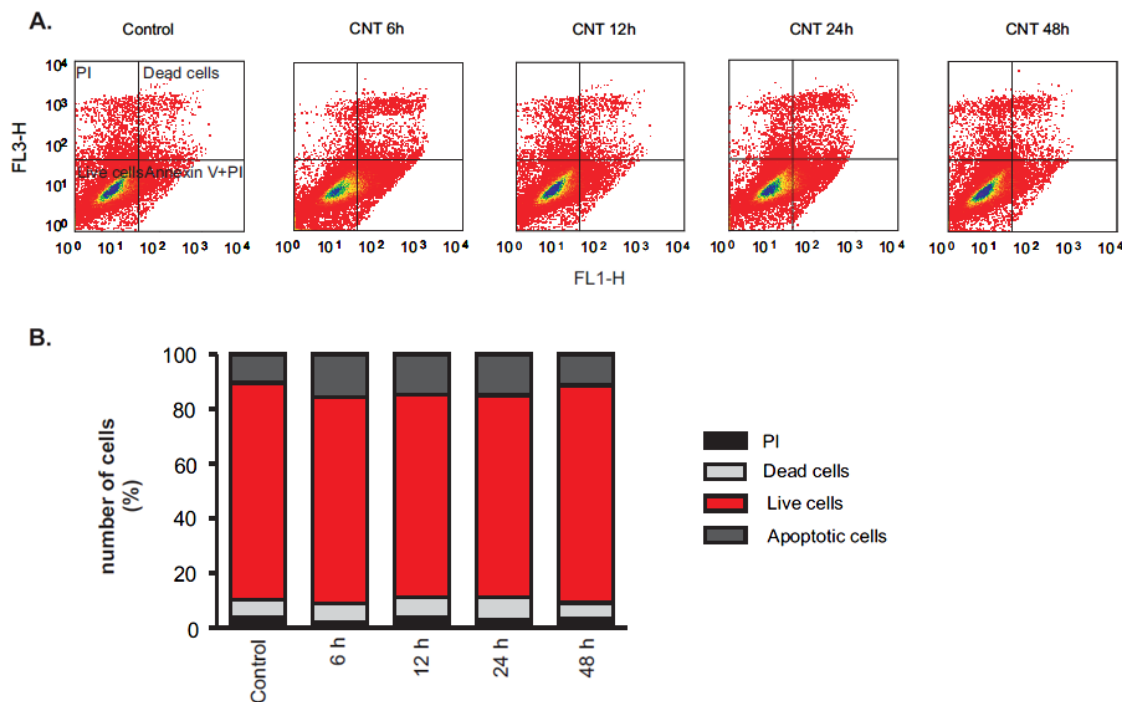


**Figure 1.** CNTs do not affect SKHeP 1 cell viability. Cellular viability was assessed by FACS in cells incubated with CNTs ( $0.025 \text{ mg ml}^{-1}$ ) for 6, 12, 24 and 48 h. (A) Representative FACS analyses shown in the histogram format. (B) Bar graph showing that SKHeP 1 cell viability is not altered by CNT exposure at different time points.

(This figure is in colour only in the electronic version)

parameters can render RNAi effects undetectable in cell culture. In order to determine the optimal time that provides maximum gene knockdown, while maintaining an acceptable level of viability for the particular cell type, we exposed cells to the CNT–siRNA–InsP3R-II complex for 2, 6, 24 and 48 h, and we performed quantitative real-time PCR experiments. Cell medium was changed to remove the transfection complex after each time point, and siRNA silencing efficiency was measured 48 h after transfection began. As shown in figure 2, higher InsP3R gene knockdown was achieved when cells were exposed to the CNT–siRNA–InsP3R-II complex for 24 and 48 h. CNTs alone did not interfere with InsP3R mRNA levels.

In order to confirm this data, we performed immunofluorescence experiments in SKHeP1 cells stained with anti-InsP3R antibodies. As shown in figure 3(A), InsP3R-II protein levels were significantly reduced in cells treated for 48 h with the CNT–siRNA–InsP3R-II complex, when compared to control untreated cells. Quantitative real-time PCR experiments also corroborated this data (figure 3(B)). We next compared the efficiency of the CNT–siRNA–InsP3R-II complex to an available commercial method (RNAifect, Qiagen). For this experiment, two different dilutions of RNAifect (3 and  $6 \mu\text{l}$ ) were used, according to the manufacturer's instructions, in conjunction with 50 or 100 nM InsP3R-II siRNA. Under these conditions significant reduction of InsP3R-II mRNA was observed (figure 3(B)). For CNT–siRNA experiments four different combinations were evaluated. All combinations led to reduced InsP3R-II mRNA levels, with higher efficiency observed in the cells transfected with the complex formed by

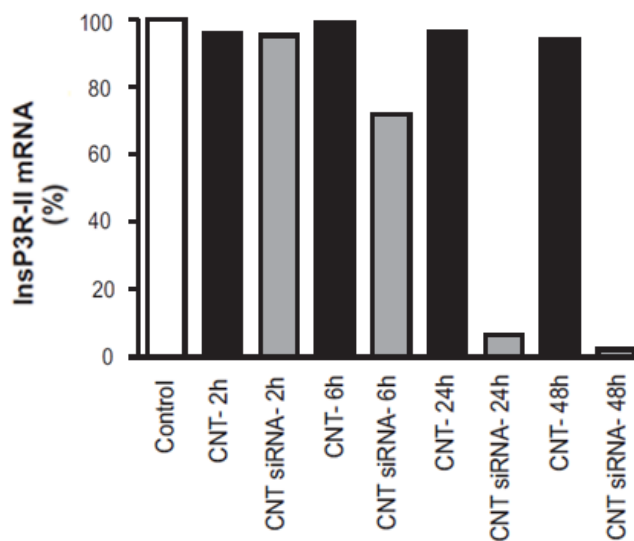


**Figure 2.** Time dependence of CNTs as siRNA carriers. Cells were incubated with transfection complex (CNT–siRNA–InsP3R-II) for 2, 6, 24 and 48 h, after which media was replaced by regular culture media. InsP3R-II mRNA levels were examined 48 h after transfection began. Significant InsP3R-II gene knockdown was observed in cells incubated with transfection complex for 24 and 48 h.

combination of 100 nM siRNA and  $0.0250 \text{ mg ml}^{-1}$  CNTs. Since type III InsP3R is also found in this cell type, we decided to assess whether our silencing complex targeted to InsP3R-II would affect InsP3R-III mRNA expression levels. As shown in

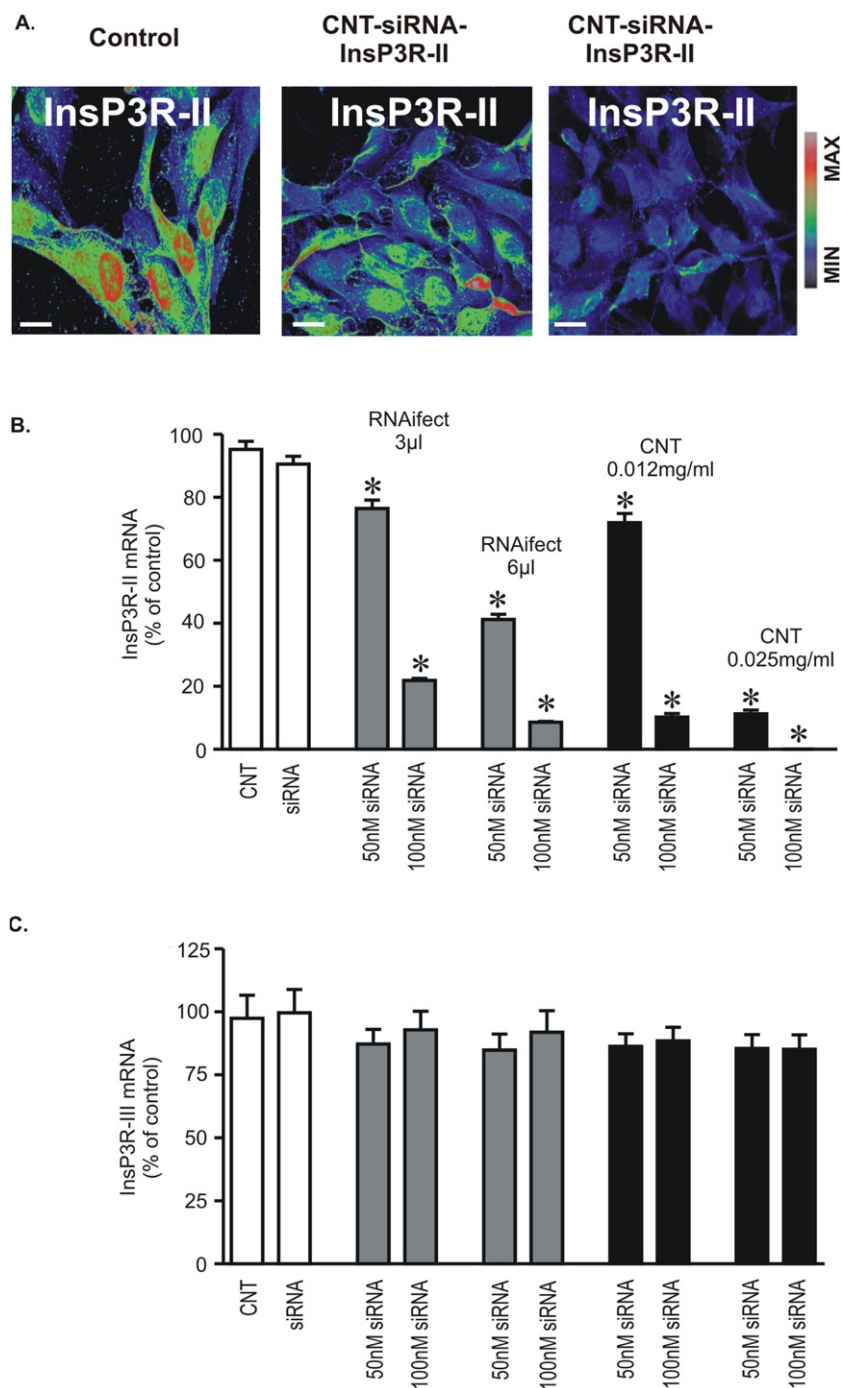


**Figure 3.** CNT–siRNA–InsP3R-II complex reduces InsP3R-II expression levels in SKHep1 cells. (A) Representative confocal images showing InsP3R-II labeled cells. InsP3R-II staining was significantly reduced in SKHep1 cells transfected with CNT–siRNA–InsP3R-II (middle and right panels) when compared to control cells (left panel). Confocal images were collected 48 h after transfection began. Final concentration of 50 nM (middle panel) or 100 nM siRNA (right panel) were efficiently delivered by CNTs in SKHep 1 cells. Images were pseudocolored according to the color scale. Scale bar = 10  $\mu$ m. (B) and (C) Real-time PCR comparing type II and type III InsP3R mRNA expression levels following siRNA transfection using CNTs or a lipid-based gene transfer system as RNA carriers. siRNA:RNAiVect reagent combination was evaluated at ratios of 50 nM:3  $\mu$ l, 100 nM:3  $\mu$ l, 50 nM:6  $\mu$ l and 100 nM:6  $\mu$ l. For CNT–siRNA complex formation different concentrations of CNT (0.0125 or 0.025 mg ml<sup>-1</sup>) were added to the diluted siRNA (50 or 100 nM final concentration). Both transfection agents were efficient in suppressing InsP3R-II gene expression in SKHep1 cells. (C) InsP3R-III transcript levels were not altered in cells transfected with InsP3R-II siRNA.

figure 3(C), InsP3R-II silencing was achieved without any impact on InsP3R-III message level. Moreover, we observed a dose dependence on silencing efficiency, since a higher CNT to siRNA ratio produced more efficient knocking down, with

no apparent impact on nonspecific gene silencing or toxicity. This finding is consistent with the idea that nanotube uptake into the cells increases as a function of nanotube concentration in the medium (Cherukuri *et al* 2004).

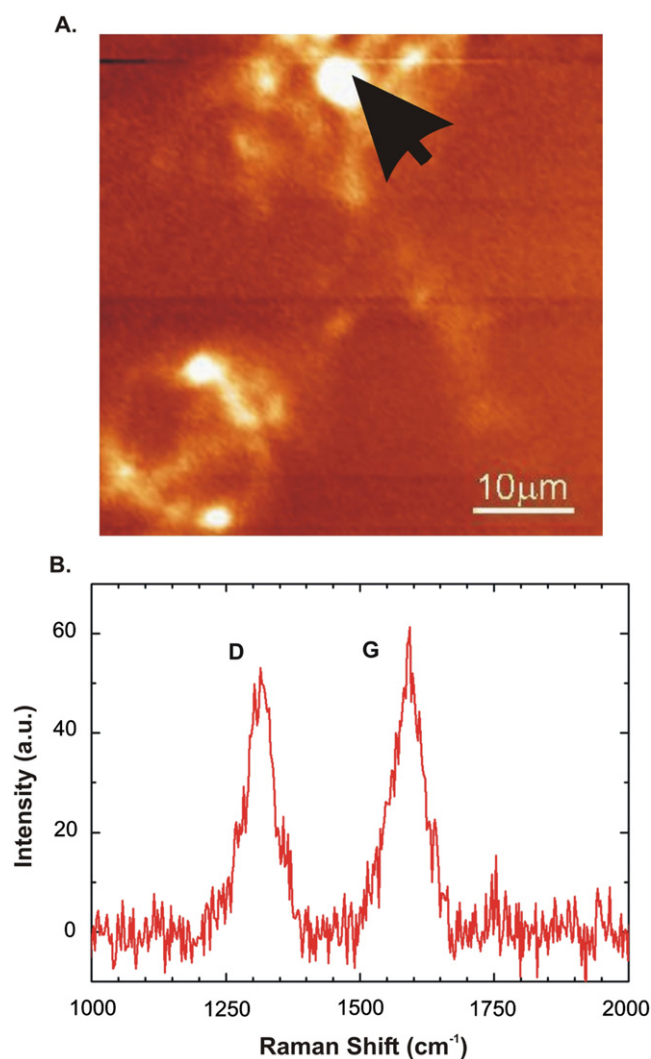


**Figure 4.** CNTs can be uptaken by neonatal cardiomyocytes. The G band Raman peak at  $1590\text{ cm}^{-1}$  was used for CNT detection in this cell. (A) The plot of the carbon nanotube G band Raman intensity (degree of yellow) gives the CNT concentration inside the neonatal cardiomyocyte. (B) Representative Raman spectrum of neonatal cardiomyocytes exposed to CNTs ( $0.025\text{ mg ml}^{-1}$ ) for 48 h taken from the area marked by the black arrow. The G and D carbon nanotube Raman peaks are highlighted.

### 3.3. Neonatal cardiomyocyte viability is not affected by internalized CNTs

In order to assess whether functionalized CNTs are also capable of carrying siRNA into neonatal cardiomyocytes, we first evaluated the internalization potential of CNTs into this cell type. Cardiomyocytes were incubated with  $0.025\text{ mg ml}^{-1}$  CNTs for 48 h and then examined by Raman spectroscopy. Figure 4 panels (A) and (B) show the presence of CNTs inside neonatal cardiomyocytes, confirming the ability of CNTs to enter this cell.

In contrast to SKHeP 1 cells that are capable of proliferating, neonatal cardiomyocytes irreversibly withdraw from the cell cycle soon after birth and lose the cell proliferative activity (Campa *et al* 2008). Therefore, to evaluate CNT effects on cellular viability we used a

fluorescence-based live/dead assay (figure 5(A)). The bar graph in figure 5(B) shows that incubation of neonatal cardiomyocytes with a higher dose of CNTs ( $0.050\text{ mg ml}^{-1}$ ) does not alter the proportion of live/dead cells when compared with untreated cells.

Neonatal cardiomyocytes beat spontaneously when maintained in culture, as a result of intracellular  $\text{Ca}^{2+}$  increase known as  $\text{Ca}^{2+}$  transient. In cardiomyocytes,  $[\text{Ca}^{2+}]_i$  transients are induced by a  $\text{Ca}^{2+}$  influx triggering a large  $\text{Ca}^{2+}$  release from the sarcoplasmic reticulum (SR) (Lukyanenko *et al* 2001). To evaluate whether CNTs affect normal physiological behavior of cardiomyocytes, we recorded  $\text{Ca}^{2+}$  transients in Fluo-4/AM loaded cells after CNT exposure (final concentration  $0.050\text{ mg ml}^{-1}$  for 48 h). As shown in figures 5(C) and (D), beating frequency was not different between neonatal cardiomyocytes treated or not with CNTs. In conclusion, no apparent change in cellular viability was observed in cardiomyocytes, even when a higher dose of CNTs was used ( $0.05\text{ mg ml}^{-1}$ ). Taken together, these data present strong evidence that CNTs can enter inside cardiomyocytes with minimal side effects to the cells.

### 3.4. Efficient *InsP3R-II* silencing in neonatal cardiomyocytes

In order to investigate whether CNTs can efficiently deliver siRNAs inside neonatal cardiomyocytes, we transfected cells with the CNT-siRNA-*InsP3R-II* complex. In cardiomyocytes *InsP3R-II* is the predominant isoform and its distribution has been reported both in the sarcoplasmic reticulum and in the nuclear region (Garcia *et al* 2004, Guatimosim *et al* 2008). We exposed cardiomyocytes to the CNT-siRNA-*InsP3R-II* complex ( $0.0250\text{ mg ml}^{-1}$  and  $100\text{ nM}$  of siRNA) and evaluated, by immunofluorescence using specific anti-*InsP3R-II* antibody, the expression levels of this receptor in the cell. As expected, *InsP3R-II* was found in the cytosol and nuclear envelope of control cells exposed to CNTs (figure 6(A)). In cells treated with the CNT-siRNA-*InsP3R-II* complex, *InsP3R-II* labeling was significantly reduced when compared to control cells. To investigate if *InsP3R-II* silencing affected the expression levels of other proteins in the cells, we analyzed the cellular distribution of another intracellular  $\text{Ca}^{2+}$  release channel in cardiomyocytes, RyR-II. RyR-II is the main  $\text{Ca}^{2+}$  release channel found in the sarcoplasmic reticulum of cardiomyocytes. In cells treated with the CNT-siRNA-*InsP3R-II* complex RyR-II immunostaining was not altered. Real-time quantitative PCR experiments corroborated these findings showing a significant silencing of *InsP3R-II* mRNA when cells were transfected with CNT-siRNA-*InsP3R-II* complex (figure 6(B)). Silencing efficiency exhibited a dose dependence since cells incubated with a higher proportion of CNTs to siRNA presented more reduced *InsP3R-II* mRNA levels. We also compared the efficiency of CNTs as an siRNA carrier to RNAiVect. CNT efficiency was almost two times higher than that obtained with the RNAiVect-siRNA-*InsP3R-II* complex (figure 6(B)). Accordingly, *InsP3R-II* silencing was achieved in neonatal cardiomyocytes without any impact on RyR-II mRNA levels (figure 6(C)). Interestingly, CNT efficiency as a transfection agent, when compared to a commercial agent, was more apparent in a hard-to-transfect cell type, such as cardiomyocytes, than in SKHeP 1 cells.



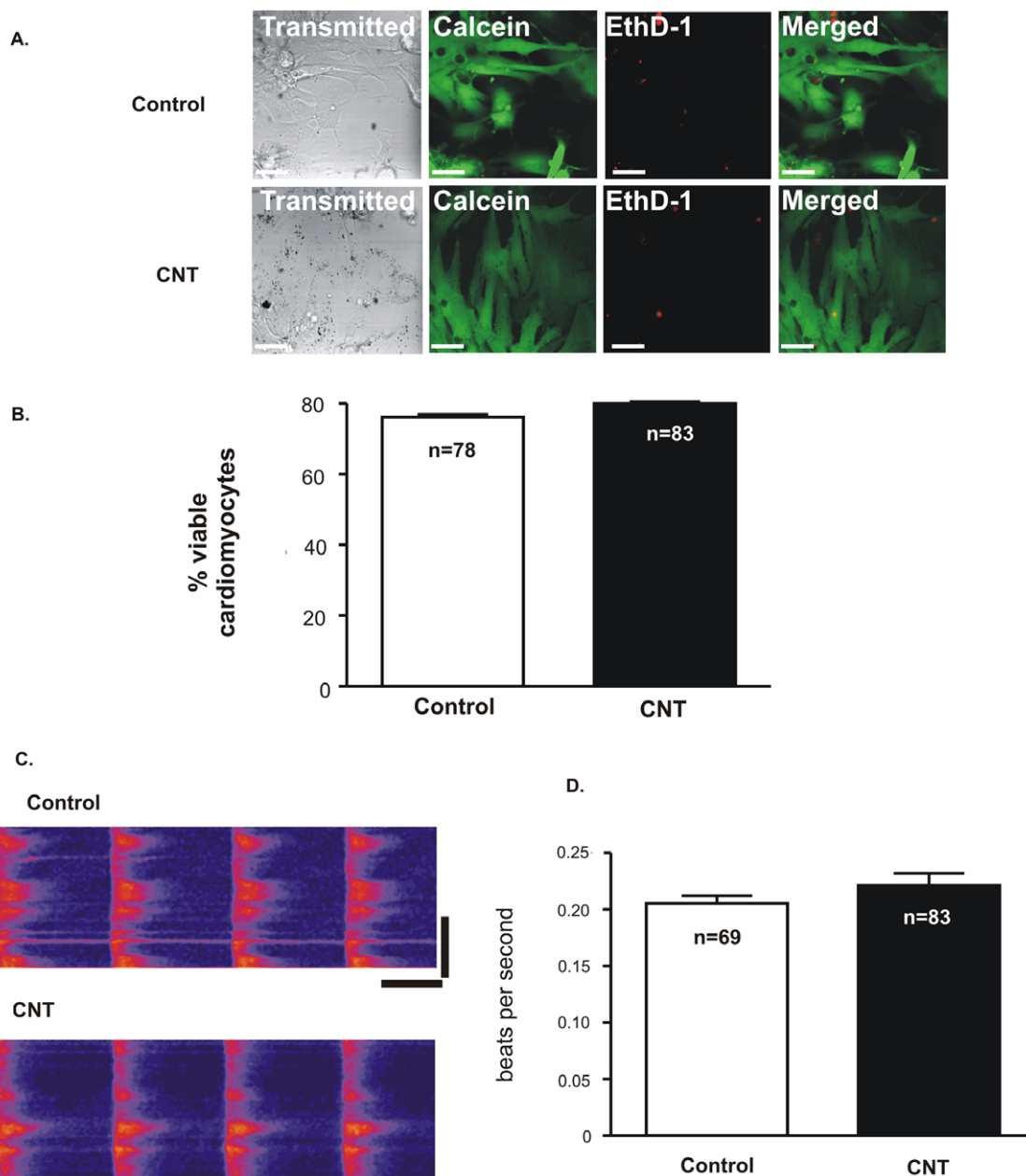


**Figure 5.** CNTs do not alter cardiomyocyte dynamics. (A) Cardiomyocytes were submitted to fluorescence-based live/dead viability assay. Dead cells were labeled with EthD-1 (red) and living cells were labeled with calcein AM (green). Images of neonatal cardiomyocytes exposed or not (untreated control) to CNTs ( $0.05 \text{ mg ml}^{-1}$ ) for 48 h were collected in a confocal microscope. (B) Averaged bar graph shows that cell viability is not altered by CNTs. Values are presented as mean  $\pm$  S.E.M. of three independent experiments.  $n$  = number of cells. (C) Representative line-scan confocal image of cells incubated or not with CNT solution. Neonatal cardiomyocyte beating frequency was monitored in Fluo-4/AM loaded cells following incubation with CNTs ( $0.05 \text{ mg ml}^{-1}$ ) for 48 h. (D) Averaged bar graph shows that CNTs do not alter cardiomyocyte beating frequency. The data shown is representative of three independent experiments.  $n$  = number of cardiomyocytes analyzed. Scale bar =  $10 \mu\text{m}$ .

### 3.5. Silencing efficiency of SWCNT-siRNA complex in DRG cells

In DRG neurons the InsP3R-I is the major isoform (Dent *et al* 1996). To evaluate the efficiency of CNTs as siRNA carriers in another hard-to-transfect cell, we performed immunofluorescence experiments in DRG neurons maintained in culture for 48 h in the presence of the CNT-siRNA-InsP3R-I complex formed by a combination of  $0.0250 \text{ mg ml}^{-1}$  CNTs

to  $100 \text{ nM}$  siRNA. As shown in figure 7(A) DRG neurons express InsP3R-I in the cytosol and in the nucleus (Dent *et al* 1996, Blackshaw *et al* 2000). Significant reduction of InsP3R-I was observed in DRG cells exposed to the CNT-siRNA-InsP3R-I complex, when compared to CNT-exposed control cells. The transmitted image presented in figure 7(B) shows the uptake of the CNT-siRNA-InsP3R-I complex by DRG neurons. Panel 7(B) shows that DRG cells retain their morphological structure in the presence of CNTs.

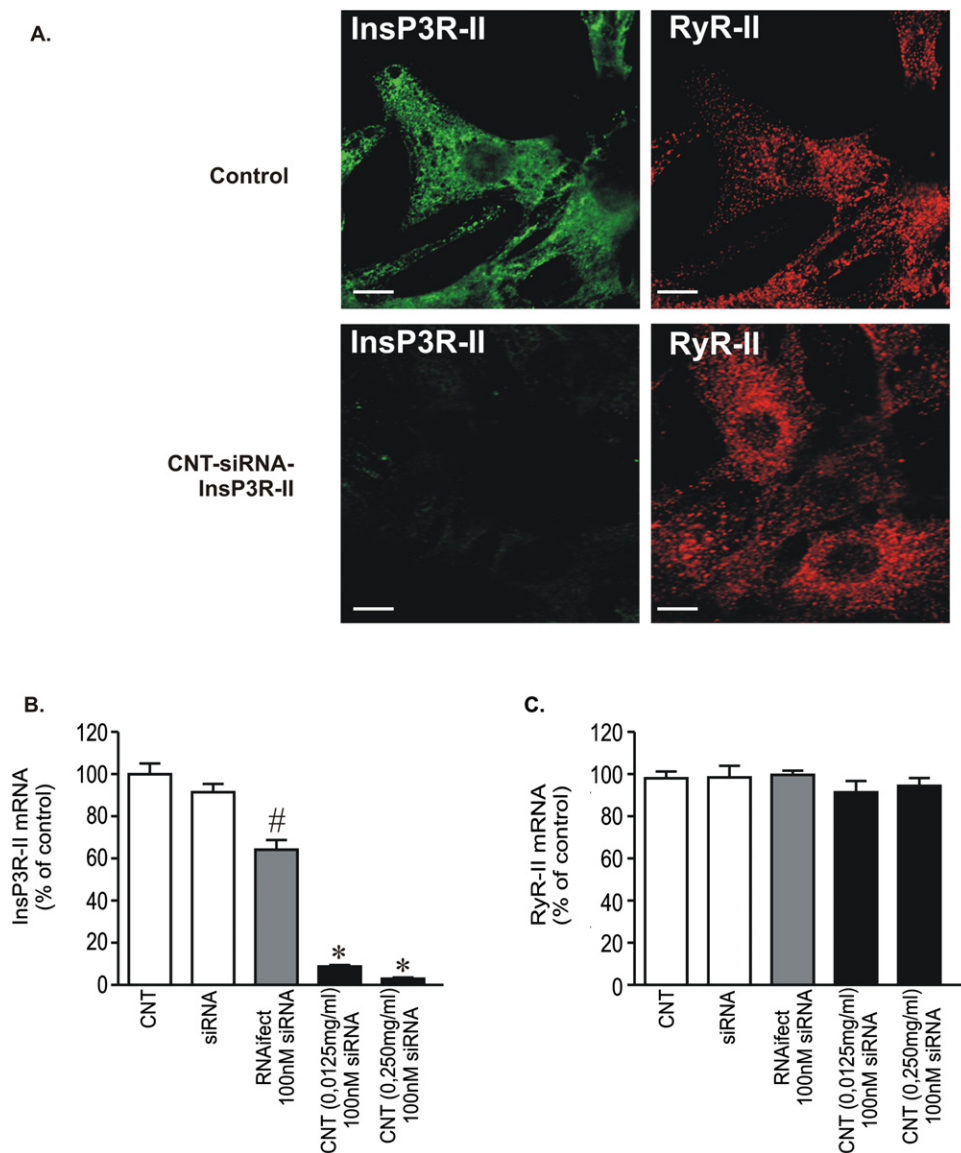


**Figure 6.** Efficient reduction of InsP3R-II expression in neonatal cardiomyocytes after CNT-siRNA-InsP3R-II complex transfection. (A) (top) Representative immunofluorescence of neonatal cardiomyocytes double-labeled with anti-InsP3R-II (green, left panel) and anti-RyR-II antibodies (red, right panel). (Bottom) Representative immunofluorescence of neonatal cardiomyocytes following transfection with CNT-siRNA-InsP3R-II complex for 48 h and double-labeled with anti-InsP3R-II (green, left panel) and anti-RyR-II antibodies (red, right panel). CNT efficiently delivered InsP3R-II siRNA (100 nM) into cardiomyocytes and reduced InsP3R-II expression in these cells. RyR-II immunolocalization was not altered in CNT-siRNA-InsP3R-II cardiomyocytes. Scale bar = 10  $\mu\text{m}$ . (B) Forty eight hours following transfection with siRNA complexed with CNT or with a lipid-based gene transfer system (RNAiAfect), cells were harvested, mRNA was isolated and real-time PCR was performed to determine the InsP3R-II expression levels. Real-time PCR assay shows that cells transfected with a combination of 3  $\mu\text{l}$  RNAiAfect and 100 nM siRNA presented a 30% reduction in InsP3R-II mRNA levels. For CNT-siRNA complex formation different concentrations of CNT (0.0125 or 0.025  $\text{mg ml}^{-1}$ ) were added to the diluted 100 nM final concentration of InsP3R-II siRNA. InsP3R-II gene was suppressed with higher efficiency in neonatal cardiomyocytes transfected with CNT-siRNA-InsP3R-II complex than with RNAiAfect. (C) RyR-II transcript levels were determined in the same samples as in (B). RyR-II mRNA expression levels were not affected by incubation with RNAiAfect or CNT-siRNA-InsP3R-II complex. The data shown are mean values  $\pm$  S.E.M of at least two independent experiments. # =  $p < 0.05$  and \* =  $p < 0.001$  when compared with control data.

#### 4. Discussion

Here we showed an examination of CNT properties by checking simultaneously its biocompatibility and efficiency as an siRNA delivery method. In this work, we were able to visualize an efficient knockdown of the siRNA target to the InsP3R isoform into three distinct cell types (DRG, neonatal

cardiomyocytes and SKHepl cells) by using purified short CNTs.

Strategies aimed to increase CNT delivery efficiency are constantly under investigation. A previous study has reported a highly efficient molecular delivery of DNA plasmid, based on the penetration of nickel-embedded CNTs into targeted cell membranes by magnetic field driving (Cai *et al* 2005). Other

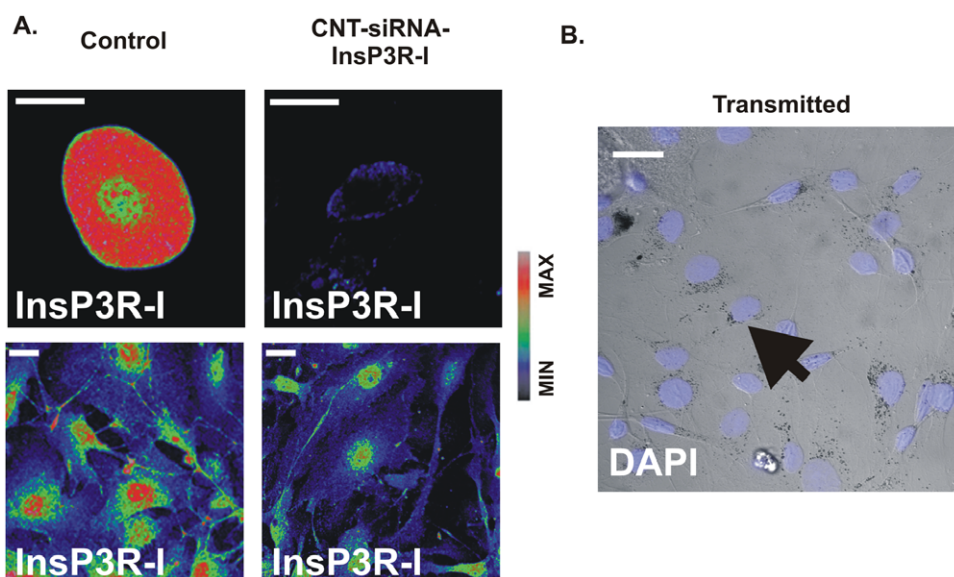


**Figure 7.** CNT–siRNA–InsP3R-I complex reduces InsP3R-I expression levels in DRG-transfected cells. (A) Immunofluorescence images of InsP3R-I labeled cells. CNT–siRNA was formed by a combination of  $0.025 \text{ mg ml}^{-1}$  CNT and  $100 \text{ nM}$  siRNA. CNTs efficiently delivered siRNA into DRG cells leading to decreased InsP3R-I expression levels. Images are pseudocolored according to the color scale. (B) Transmitted image of DRG cells showing the presence of CNT in the cytoplasm (arrow). Cell nucleus was labeled with Dapi (blue). Scale bar =  $10 \mu\text{m}$ .

groups have also used different strategies to deliver siRNA into mammal cells by chemically modifying CNTs with groups that could be covalently or electrostatically linked to the siRNA (Kam *et al* 2005, Rege *et al* 2006, Zhang *et al* 2006, Krajcik *et al* 2008). In fact, it has been shown that positively charged CNTs successfully mediate targeted gene interference when complexed with an siRNA concentration of  $2 \text{ nM}$  (Zhang *et al* 2006). While these approaches were efficient, they required complex modifications of the CNTs, which may have increased contamination with residues. Furthermore, most of these studies used immortalized cell lines that, in general, are considered easy to transfect (Kam *et al* 2005). The delivery efficiency presented by CNTs can be explained, at least in part, by its larger aspect ratio when compared to classical delivery systems, such as liposomes. It allows for more siRNA load and more efficient permeation through cell membranes (Kam and Dai 2006). In fact, CNTs can efficiently deliver siRNA into human T-cells and microglia, whereas conventional transfection vectors such as lipofectamine show little effect in the internalization of siRNA in these cell types (Liu *et al* 2007, Kateb *et al* 2007). A dependence of the delivery ability of nanotubes on functionalization and the degree of hydrophilicity has been reported previously (Liu *et al* 2007). Accordingly, hydrophobic interactions are an underlying factor in nanotube-mediated molecular delivery, suggesting that a balanced chemical functionalization should be achieved in order to handle solubility without impairing their ability to enter inside the cell (Liu *et al* 2007).

Although the biological effects of CNTs still remain unclear, evidence in support of non-cellular toxicity of CNTs is found in the literature (Shi Kam *et al* 2004, Pantarotto *et al* 2004, Zhang *et al* 2006, Liu *et al* 2007, Cui *et al* 2007, Dumortier *et al* 2006, Kateb *et al* 2007). In this study

we expanded this data by showing that CNTs do not affect cellular viability in spite of changing gene expression levels of important cellular pro-apoptotic genes and cell cycle regulators in SKHep 1 cells. However, we also noted a higher expression of survival genes, which may have compensated the increased expression of death genes. This data was confirmed by FACS, which showed no effect of CNTs on SKHep 1 cells viability. These data correlated with findings from a previous study (Shi Kam *et al* 2004) showing that the uptake of SWCNTs did not adversely affect HL60 cells at equivalent CNT concentration used in this work. No apparent change in cellular viability was also observed in cardiomyocytes, even when a higher dose of CNTs was used ( $0.05 \text{ mg ml}^{-1}$ ). Two lines of evidence support this assumption: (i) cardiomyocyte beating rate was not affected by CNT exposure and (ii) live/dead experiments indicated that exposure of cardiomyocytes to CNTs did not alter the percentage of live cells. This data is in line with a previous report showing a lack of toxicity of functionalized CNTs in cardiomyocytes (Krajcik *et al* 2008). Besides RyR immunolabeling or mRNA levels were similar in cardiomyocytes treated or not with CNTs.

Another important issue is the location of CNTs inside the cells. By using fluorescence microscopy, it has been reported the presence of CNTs inside phagosomes of a macrophage-like cell, with no apparent toxicity (Cherukuri *et al* 2004). Although some reports described that CNTs can enter the nucleus, its presence in the nucleus is still controversial (Mu *et al* 2009). We have observed the presence of CNTs in the cytosol of all cells studied, although the specific localization was not determined. More work is necessary in order to answer this question.

Surprisingly, 96% silence of the expression of InsP3R-II was achieved in cardiomyocytes, an amount which was

never reached by a commercially available method, until now. Moreover, we observed an efficient gene silencing by increasing the ratio of CNTs to siRNA, with no apparent impact on nonspecific gene silencing or toxicity. This finding is consistent with the idea that nanotube uptake into the cells increases as a function of nanotube concentration in the medium (Cherukuri et al 2004).

Different from our work, CNT preparations generally using side groups containing large carbon strain make siRNA binding to CNTs difficult. Furthermore, the increase in the number of positive charges on the CNT surface may cause a strong interaction between siRNA and CNTs, which may cause the release of siRNA from the complex difficult once inside the cell. The use of siRNA carriers based on short single-wall CNTs (length 50–500 nm) with just a few chemical groups such as COOH– or NH<sub>3</sub>– is expected to overcome these problems by achieving three major goals: reduction of toxicity, enhancement of the stability of siRNA and increase of siRNA permeation into cells. In addition, CNT efficiency as a transfection agent was more apparent in a hard-to-transfect cell type, such as cardiomyocytes, than in SKHeP 1 cells.

In conclusion, short single-wall carboxylated-CNT–siRNA represents a very effective RNAi carrier to different cell types, providing an efficient silencing of the target gene with high specificity and large reduction in toxicity.

## Acknowledgments

This work was supported by Instituto do Milênio/CNPq–MCT, Instituto Nacional de Ciência e Tecnologia de Nanomateriais de Carbono–CNPq (Conselho Nacional de Desenvolvimento Científico e Tecnológico) and Rede Mineira de Biotecnologia e Bioensaios (FAPEMIG), Brazil. RRR, SG, RGL, MFL and LOL are grateful for grants from CNPq (Conselho Nacional de Desenvolvimento Científico e Tecnológico) and FAPEMIG (Fundação de Amparo à Pesquisa do Estado de Minas Gerais), Brazil. We also would like to thank Bernardo R A Neves for the AFM measurements and Débora Pereira for helping with the functionalization experiments. MSL is a recipient of a CAPES PhD fellowship at the Post-graduation Program in Biological Science: Physiology and Pharmacology at UFMG.

## References

- Blackshaw S, Sawa A, Sharp A H, Ross C A, Snyder S H and Khan A A 2000 Type 3 inositol 1,4,5-trisphosphate receptor modulates cell death. *FASEB J.* **14** 1375–9
- Cai D, Mataraza J M, Qin Z H, Huang Z, Huang J, Chiles T C, Carnahan D, Kempa K and Ren Z 2005 Highly efficient molecular delivery into mammalian cells using carbon nanotube sparring. *Nat. Methods* **2** 449–54
- Campa V M, Gutierrez-lanza R, Cerignoli F, Diaz-trelles R, Nelson B, Tsuji T, Barcova M, Jiang W and Mercola M 2008 Notch activates cell cycle reentry and progression in quiescent cardiomyocytes. *J. Cell Biol.* **183** 129–41
- Cherukuri P, Bachilo S M, Litovsky S H and Weisman R B 2004 Near-infrared fluorescence microscopy of single-walled carbon nanotubes in phagocytic cells. *J. Am. Chem. Soc.* **126** 15638–9
- Cherukuri P, Gannon C J, Leeuw T K, Schmidt H K, Smalley R E, Curley S A and Weisman R B 2006 Mammalian pharmacokinetics of carbon nanotubes using intrinsic near-infrared fluorescence. *Proc. Natl Acad. Sci. USA* **103** 18882–6
- Cui D, Tian F, Coyer S R, Wang J, Pan B, Gao F, He R and Zhang Y 2007 Effects of antisense-myc-conjugated single-walled carbon nanotubes on HL-60 cells. *J. Nanosci. Nanotechnol.* **7** 1639–46
- Da Silva E E, Della Colleta H H M, Ferlauto AS, Moreira R L, Resende R R, Oliveira S, Kitten G T, Lacerda R G and Ladeira L O 2009 Nanostructured 3D collagen/nanotube biocomposites for future bone regeneration scaffolds. *Nano Res.* **2** 462–73
- Dent M A, Raisman G and Lai F A 1996 Expression of type 1 inositol 1,4,5-trisphosphate receptor during axogenesis and synaptic contact in the central and peripheral nervous system of developing rat. *Development* **122** 1029–39
- Dubin R A, Callegari G, Kohn J and Neimark A 2008 Carbon nanotube fibers are compatible with mammalian cells and neurons. *IEEE Trans. Nanobiosci.* **7** 11–4
- Dumortier H, Lacotte S, Pastorin G, Marega R, Wu W, Bonifazi D, Briand J P, Prato M, Muller S and Bianco A 2006 Functionalized carbon nanotubes are non-cytotoxic and preserve the functionality of primary immune cells. *Nano Lett.* **6** 1522–8
- Echevarria W, Leite M F, Guerra M T, Zipfel W R and Nathanson M H 2003 Regulation of calcium signals in the nucleus by a nucleoplasmic reticulum. *Nat. Cell Biol.* **5** 440–6
- Garcia K D, Shah T and Garcia J 2004 Immunolocalization of type 2 inositol 1,4,5-trisphosphate receptors in cardiac myocytes from newborn mice. *Am. J. Physiol. Cell Physiol.* **287** C1048–57
- Guatimosim S et al 2008 Nuclear Ca(2+) regulates cardiomyocyte function. *Cell Calcium* **44** 230–42
- Hagar R E, Burgstahler A D, Nathanson M H and Ehrlich B E 1998 Type III InsP3 receptor channel stays open in the presence of increased calcium. *Nature* **396** 81–4
- Kam N W, Liu Z and Dai H 2005 Functionalization of carbon nanotubes via cleavable disulfide bonds for efficient intracellular delivery of siRNA and potent gene silencing. *J. Am. Chem. Soc.* **127** 12492–3
- Kam N W S and Dai H 2006 Single walled carbon nanotubes for transport and delivery of biological cargos. *Phys. Status Solidi b* **243** 3561–6
- Kateb B, Van handel M, Zhang L, Bronikowski M J, Manohara H and Badie B 2007 Internalization of MWCNTs by microglia: possible application in immunotherapy of brain tumors. *Neuroimage* **37** (suppl 1) S9–17
- Krajcik R, Jung A, Hirsch A, Neuhuber W and Zolk O 2008 Functionalization of carbon nanotubes enables non-covalent binding and intracellular delivery of small interfering RNA for efficient knock-down of genes. *Biochem. Biophys. Res. Commun.* **369** 595–602
- Leite M F, Hirata K, Pusch T, Burgstahler A D, Okazaki K, Ortega J M, Goes A M, Prado M A, Spray D C and Nathanson M H 2002 Molecular basis for pacemaker cells in epithelia. *J. Biol. Chem.* **277** 16313–23
- Liu Z, Davis C, Cai W, He L, Chen X and Dai H 2008 Circulation and long-term fate of functionalized, biocompatible single-walled carbon nanotubes in mice probed by Raman spectroscopy. *Proc. Natl Acad. Sci. USA* **105** 1410–5
- Liu Z, Winters M, Holodniy M and Dai H 2007 siRNA delivery into human T cells and primary cells with carbon-nanotube transporters. *Angew. Chem. Int. Edn Engl.* **46** 2023–7
- Lukyanenko V, Viatchenko-Karpinski S, Smirnov A, Wiesner T F and Gyorke S 2001 Dynamic regulation of sarcoplasmic reticulum Ca(2+) content and release by luminal Ca(2+)-sensitive leak in rat ventricular myocytes. *Biophys. J.* **81** 785–98
- Mendes C C, Gomes D A, Thompson M, Souto N C, Goes T S, Goes A M, Rodrigues M A, Gomez M V, Nathanson M H and Leite M F 2005 The type III inositol 1,4,5-trisphosphate receptor preferentially transmits apoptotic Ca2+ signals into mitochondria. *J. Biol. Chem.* **280** 40892–900

- Mu Q, Broughton D L and Yan B 2009 Endosomal leakage and nuclear translocation of multiwalled carbon nanotubes: developing a model for cell uptake *Nano Lett.* **9** 4370–5
- Pantarotto D, Briand J P, Prato M and Bianco A 2004 Translocation of bioactive peptides across cell membranes by carbon nanotubes *Chem. Commun. (Camb)* **16**–7
- Rege K, Viswanathan G, Zhu G, Vijayaraghavan A, Ajayan P M and Dordick J S 2006 *In vitro* transcription and protein translation from carbon nanotube–DNA assemblies *Small* **2** 718–22
- Resende R R, Gomes K N, Adhikari A, Britto L R and Ulrich H 2008 Mechanism of acetylcholine-induced calcium signaling during neuronal differentiation of P19 embryonal carcinoma cells *in vitro Cell Calcium* **43** 107–21
- Shi Kam N W, Jessop T C, Wender P A and Dai H 2004 Nanotube molecular transporters: internalization of carbon nanotube–protein conjugates into mammalian cells *J. Am. Chem. Soc.* **126** 6850–1
- Soares F A, Segundo G R, Alves R, Ynoue L H, Resende R O, Sopelete M C, Silva D A, Sung S S and Taketomi E A 2007 Indoor allergen sensitization profile in allergic patients of the allergy clinic in the University Hospital in Uberlandia, Brazil *Rev. Assoc. Med. Bras.* **53** 25–8
- Trigueiro J P et al 2007 Purity evaluation of carbon nanotube materials by thermogravimetric, TEM, and SEM methods. *J. Nanosci. Nanotechnol.* **7** 3477–86
- Wojcikiewicz R J 1995 Type I, II, and III inositol 1,4,5-trisphosphate receptors are unequally susceptible to down-regulation and are expressed in markedly different proportions in different cell types *J. Biol. Chem.* **270** 11678–83
- Zhang Z, Yang X, Zhang Y, Zeng B, Wang S, Zhu T, Roden R B, Chen Y and Yang R 2006 Delivery of telomerase reverse transcriptase small interfering RNA in complex with positively charged single-walled carbon nanotubes suppresses tumor growth *Clin. Cancer Res.* **12** 4933–9